J Solid State Electrochem (2006) 10: 348–359
DOI 10.1007/s10008-005-0683-5

ORIGINAL PAPER

Hamid R. Zare · Ali M. Habibirad

Electrochemistry and electrocatalytic activity of catechin film on a glassy carbon electrode toward the oxidation of hydrazine

Received: 25 January 2005 / Revised: 12 March 2005 / Accepted: 1 April 2005 / Published online: 30 June 2005

Abstract A very stable electroactive film of catechin was electrochemically deposited on the surface of activated glassy carbon electrode. The electrochemical behavior of catechin modified glassy carbon electrode (CMGCE) was extensively studied using cyclic voltammetry. The properties of the electrodeposited films, during preparation under different conditions, and the stability of the deposited film were examined. The charge transfer coefficient (α) and charge transfer rate constant (k_s) for catechin deposited film were calculated. It was found that the modified electrode exhibited excellent electrocatalytic activity toward hydrazine oxidation and it also showed a very large decrease in the overpotential for the oxidation of hydrazine. The CMGCE was employed to study electrocatalytic oxidation of hydrazine using cyclic voltammetry, rotating disk voltammetry, chronoamperometry, amperometry and square-wave voltammetry as diagnostic techniques. The catalytic rate constant of the modified electrode for the oxidation of hydrazine was determined by cyclic voltammetry, chronoamperometry and rotating disk voltammetry and was found to be around 10^{-3} cm s^{-1}. In the used different voltammetric methods, the plot of the electrocatalytic current versus hydrazine concentration is constituted of two linear segments with different ranges of hydrazine concentration. Furthermore, amperometry in stirred solution exhibits a detection limit of 0.165 μM and the precision of 4.7% for replicate measurements of 40.0 μM solution of hydrazine.

Keywords Hydrazine · Electrocatalytic measurement · Catechin · Modified electrode · Amperometric determination

H. R. Zare (✉) · A. M. Habibirad
Department of Chemistry, Yazd University,
Yazd, 89195-741, Iran
E-mail: hrzare@yazduni.ac.ir
Fax: +98-351-7250110

Introduction

Hydrazine is volatile and toxic and is readily absorbed by oral, dermal or inhalation routes of exposure. Adverse health effects caused by hydrazine on people living near hazardous waste sites have been described [1]. Contact with hydrazine irritates the skin, eyes and respiratory track. It is also used as an oxygen scavenger for corrosion control in boilers [2] and has found wide application as antioxidant, photographic developer, polymers, pesticides, plant-growth regulators, pharmaceuticals and insecticides [3]. Moreover, hydrazine was used as fuel in the fuel cells and as rocket fuel, due to its high capacity and no contamination [4]. Thus, there has been an increasing demand for a highly sensitive method for determination of hydrazine in various samples. Numerous methods have been reported in the literatures for the determination of hydrazine [5–8].

Potentiometric methods based on reactions of hydrazine and detection at different ion selective electrodes have also been reported [9]. Unfortunately, the electrochemical oxidation of hydrazine is found to be irreversible at ordinary carbon electrodes and requires high overvoltage [10]. To avoid these problems, many attempts have been made to reduce this high overvoltage. This high overpotential could be decreased by depositing a mediator at the electrode surface [11–18]. Electron transfer mediators have been receiving considerable attention in recent years. The main advantage in this approach is that it is possible to choose lower working potentials, characteristic of the mediator to avoid interface from other electroactive species present in the medium. In other words, electrode surface modification has been tried as a means to reduce the overvoltage and overcome the slow kinetics of many processes. Some chemically modified electrodes were constructed with good catalytic activity toward the electrooxidation of hydrazine, including cobalt phetalocyanine [11], rhodium [12], magnetic microsphere [13], ruthenium (III) [14], cobalt hexacyanoferrate [15] and

prussian blue [16]. It is generally, accepted that *o*-hydroquinones can be quite active in the electrocatalytic oxidation of hydrazine and as result, several surface modified electrodes with compounds having an *o*-hydroquinone moiety have been reported [17–18].

Recently, the preparation of catechin modified glassy carbon electrode and its use in the electrocatalysis of dopamine oxidation was reported [19]. The modification was achieved by adsorption of catechin at an electrochemically pre-treated glassy carbon electrode. Catechin is a derivative of *o*-hydroquinone with anti-cancer, anti-viral and anti-inflammatory activity, which are the consequence its affinity for proteins and their antioxidant properties [20]. It is one of the bioactive flavonoid compounds, which are found in plants [21]. Owing to the high reactivity of naturally occurring mediators, it appears that the use of catechin as modifier could be important and could yield some new information about the catalysis of slow reactions. Accordingly, in the present work, we describe the preparation and characterization of glassy carbon electrode modified with catechin and its electrocatalytic activity toward hydrazine oxidation. A glassy carbon surface was chosen for modification, since it offers a high stability, reproducibility and, due to its low cost, high suitability for a possible industrial application. Our findings indicate that the CMGCE shows a significant decrease in the overpotential of hydrazine oxidation compared with other modified electrodes [11–18].

Experimental

Chemicals

(+)-Catechin hydrate (*trans*-3,3′,4,4′,5,7-pentahydroxy flavane), see inset of Fig. 2 for structure, was purchased from Fluka and used without further purification. Hydrazine and all other chemical reagents used for buffer solutions preparation were analytical reagent grade from Merck and used as received. The buffer solutions (0.15 M) were made up from H_3PO_4 and adjusting the pH with 2.0 M NaOH. All aqueous solutions were made with doubly distilled water.

Apparatus

The Autolab potentiostate PGSTAT 30 (Echochemie, Utrecht, Netherlands), connected to a personal computer for data acquisition and potential control was used for electrochemical measurement. A single compartment cell with a three electrode configuration was used. A graphite electrode directly immersed in the solution was used as auxiliary electrode in voltammetric measurements. The working electrode used in the voltammetric experiment was a glassy carbon disk (2.0 mm diameter), which was modified as mentioned below. All potentials were referred to the saturated calomel electrode (SCE) as reference electrode. All electrodes were from Azar electrode, Iran. All experiments were carried out inside a Faraday cage at room temperature (ca. 25°C). pH was measured with a Metrohm model 691 pH/mV meter.

Modified electrode preparation

Prior to the electrode modification, the surface of glassy carbon electrode was hand-polished with 0.05 μM alumina in water slurry using a polishing cloth and then rinsed with doubly distilled water. The glassy carbon electrode was then pretreated in 0.1 M sodium bicarbonate solution with cyclic voltammetry in potential range from −1.1 V to 1.6 V at a scan rate of 100 mV s^{-1} by 16 scan. For modification, the activated electrode was rinsed with doubly distilled water and was placed in a 1.0 mM solution of catechin in 0.15 M phosphoric acid (pH = 1.5), and it was modified by eight cycles of potential sweep between 300 mV and 700 mV at 10 mV s^{-1}. Subsequently, the modified electrode was rinsed with water and placed in buffer solution (pH = 7.0). The potential was scanned for 100 potential cycling between −75 mV and 425 mV at 100 mV s^{-1} so as to obtain a stable redox response for surface-immobilized film of catechin. Surface coverage of modified electrode was determined from the integration of charge under cyclic voltammograms, recorded at low scan rate, assuming an *n* value of 2.

Results and Discussion

The optimum conditions for preparation of catechin modified glassy carbon electrode

The effects of different experimental variables in the immobilization of catechin were investigated to optimize testing performance. In this direction, the effect of the sweep potential range, the modifier solution pH, the number of potential recycling and the catechin solution concentration during the modification step were examined. In these studies, the electrode coverage was used as a measure of surface deposited catechin and results are illustrated in Fig. 1. In all cases, the surface coverage was evaluated from the cyclic voltammograms recorded at 20 mV s^{-1} and using the equation $\Gamma = Q/nFA$, where Q is the charge obtained by integrating the anodic peak under the background correction and the other symbols have their usual meanings. However, assuming that no interaction can exist between the variables, the on-at-a-time procedure [22] was used for optimization.

The effect of the sweep potential range on the surface coverage was investigated by changing the potential extent during the modification step and the results are shown in Fig. 1a. In Fig. 1a, the pH, number of cycles and sweep rate of potential were 1.5, 4 and 10 mV s^{-1}, respectively. Based on the results illustrated in Fig. 1a,

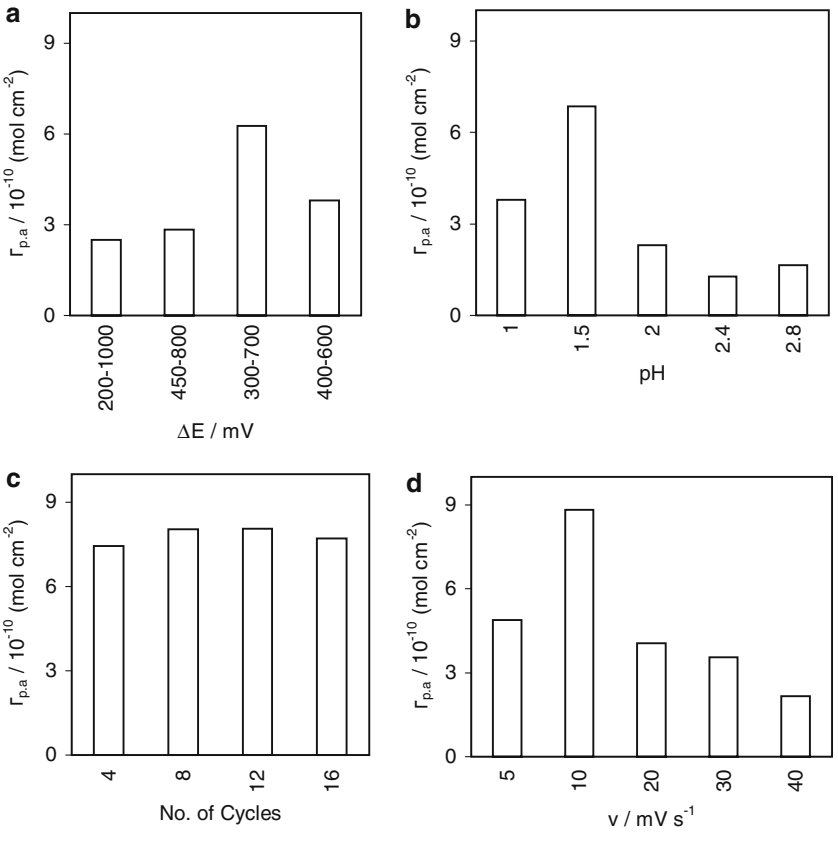

Fig. 1 Variation in anodic peak surface coverage as a function of **a** range of sweep potential, **b** Catechin solution pH, **c** sweep number of potential cycles and **d** potential sweep rates during the modification step. The anodic surface coverage was measured for second potential recycling. For the details see text

modification by cycling the potential between 300 mV and 700 mV was found as optimal and used in all subsequent studies. Figure 1b shows the effect of modifier solution pH on the electrode surface coverage. As can be seen, the best coverage was obtained when the modification was carried out in catechin solution with pH = 1.5 (0.15 M phosphoric acid); therefore, this pH was selected as optimum pH values in the subsequent modification process. It seems that at pH < 1.5, the protonation of preactivated glassy carbon electrode surface functional groups inhibits the nucleophilic reaction between the latter groups and oxidized form of catechin [11]. At pH higher than the optimum value, the oxidation product of catechin can enter in a hydroxylation reaction which minimizes the apparent reactivity of functional groups at the surface of electrode. In other words, at higher pH because of competing effect of interfering molecules reacting as nucleophiles with the oxidized form of catechin, the bond formation between the later compound and active groups at the electrode surface being to decrease [23–24]. Thus, pH = 1.5 is the optimum value for attachment modifier to the surface of glassy carbon electrode within a Michel addition process. The effect of the potential cycle number on the surface coverage of electrode was also determined. Figure 1c shows that the variations in the surface coverage of electrode for 4–16 cycles were not dramatic. However, it was found that the best results, including reproducibility of voltammograms, were obtained for electrode prepared by eight cycles of potential. Therefore, eight cycles of potential for the electrode modification was selected as optimum number and used in the next study. Finally, the effect of the sweep rate, used for surface modification, on the surface coverage was investigated. Based on the results illustrated in Fig. 1d, the best results were obtained for slow sweeping (5–10 mV s^{-1}) of potential. However, for the higher sweep rates (20–40 mV s^{-1}) a significant decrease in the surface coverage is observed. It seems that at higher scan rates the available time window is not large enough for complete deposition of modifier. Thus, a sweep rate of 10 mV s^{-1} was chosen for optimal. Based on these results, the optimal values for potential extent, pH, number of sweep rate and sweep rate of potential have been achieved to be 300–700 mV, 1.5, 8 and 10 mV s^{-1}, respectively.

Stability of the modified electrode

The stability of the CMGCE prepared under optimal conditions were examined either by potential recycling in 0.15 M phosphate buffer, pH = 7.0 (Fig. 2, curve a) or by keeping the modified electrode in 0.15 M phosphoric acid, pH = 1.5, for period of time (Fig. 2, curve b), and then recording the cyclic voltammograms in phosphate buffer, pH = 7.0. Figure 2 shows that in two cases, the surface coverage decreases

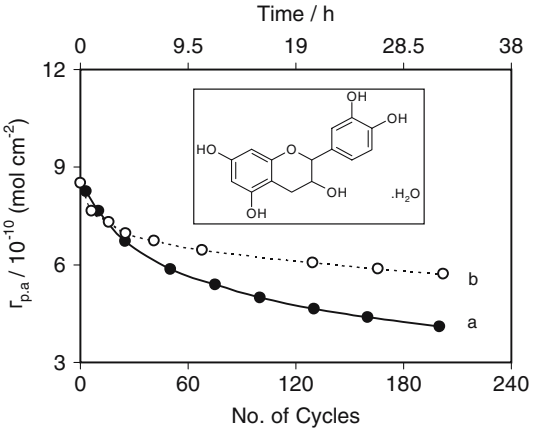

Fig. 2 Variation in anodic peak surface coverage of CMGCE prepared under optimal conditions as a function of **a** the repetitive recycling in 0.15 M phosphate buffer (pH = 7.0) and **b** the storage time of the modified electrode in 0.15 M phosphoric acid (pH = 1.5). *Inset* shows the catechin hydrate structure

rapidly at first and then remain almost constant. These results suggest that the initial decay might be due to catechin that is weakly bonded to the electrode surface, so that it can be displaced easily. In addition, investigations are shown that at high pH, the bond formed between the oxidized form of catechin and active groups at the electrode surface begin to break because of a competing effect of interfering molecules which can react as nucleophiles, instead of surface active groups, with surface bonded oxidized form of catechin. Note that, despite the diminution of electrode coverage during the potential recycling, its efficiency (defined as I_p/Γ) increases gradually until reaching a constant value.

Voltammetric properties of the catechin modified electrode

When an activated glassy carbon electrode is used as the bed for electro-oxidation of catechin, carboxyl and hydroxy groups on the activated surface of the electrode [25], behave as nucleophiles against the *o*-quinone formed from catechin oxidation. Such a process leads to bond formation between catechin and surface active groups and hence to the deposition of catechin at the electrode surface. Cyclic voltammograms of the CMGCE, prepared at the optimal conditions, in 0.15 M phosphate buffer solution (pH = 7.0) at various scan rates are shown in Fig. 3a. The electrochemical responses of the CMGCE were those anticipated for a surface-confined redox couple and the separation between anodic and cathodic peaks (ΔE_p) was 89 mV for sweep rate 100 mV s^{-1}.

A plot of peak current (I_p) versus the scan rate (v) for CMGCE shows a linear relation up to 100 mV s^{-1} as predicted theoretically for a surface-immobilized redox couples (Fig. 3b). Above 150 mV s^{-1}, the relationship becomes linear only when plotted versus the square root of v (Fig. 3c). Figure 4 shows, the plot of peak potentials versus logarithm of the potential scan rate. As mentioned above, the relationship between the peak current and the scan rate is linear only at low scan rate. In this range the surface redox reaction of bonded catechin is apparently reversible and the peak potentials are almost independent of the scan rate. At high scan rates, the separation between peak potentials increase with increasing scan rates (Fig. 4a). This is the range in which the reaction appears quasireversible and irreversible [26], and the dependence of peak currents on the scan rate declines from the linearity. i.e. the increase of peak currents with scan rates is

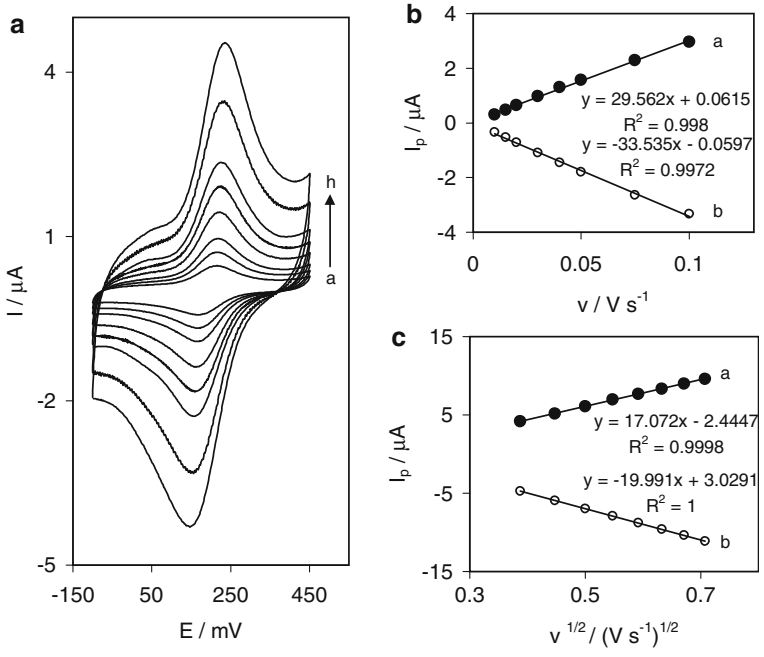

Fig. 3 **a** Cyclic voltammograms of CMGCE in 0.25 M phosphate buffer (pH = 7.0) at various scan rates. The *a* to *h* letters correspond to 10, 15, 20, 30, 40, 50, 75, 100 mV s^{-1} scan rates, respectively. Variation of $I_{p,a}$ (*curve a*) and $I_{p,c}$ (*curve b*) with **b** the scan rate and **c** the square root of scan rate

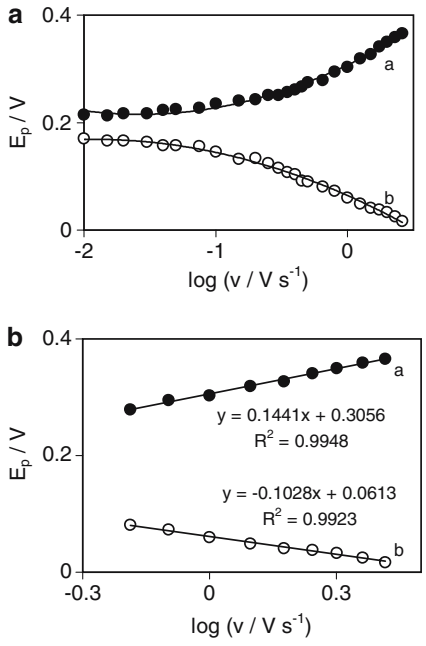

Fig. 4 **a** Variation of $E_{p,a}$ (*curve a*) and $E_{p,c}$ (*curve b*) versus the logarithm of the scan rate for a CMGCE in 0.15 M phosphate buffer (pH = 7.0). **b** Magnification of the same plot for high scan rates

lower than in the range of low scan rates. A similar observations has been reported previously for the other surface immobilized species [27, 28].

In addition, the formal potential, $E^{0'}$, is about 180 mV and is almost independent of the potential scan rate for sweep rates ranging from 10 mV s^{-1} to 400 mV s^{-1}. The formal potentials are obtained from the equation $E^{0'} = E_{p,a} - \alpha(E_{p,a} - E_{p,c})$ [29] and considering $\alpha = 0.58$ (see below). The transfer coefficient, α, and the apparent heterogeneous charge transfer rate constant, k_s, for electron transfer between the electrode and a surface-confined redox couple can be evaluated in cyclic voltammetry from the variation of the anodic and cathodic peak potentials with the logarithm of the scan rates, according to the method described by Laviron [30].

Figure 4a shows the magnitudes of peak potentials, E_p, as a function of logarithm of the potential scan rate. For high scan rates, theory predicts a linear dependence of E_p upon log(v), which can be used to extract the kinetic parameters α_a ($\alpha_a = 1 - \alpha_c$), α_c (anodic and cathodic transfer coefficients) and k_s from the slope and intercept of such plots, respectively. We have found that for scan rates above 800 mV s^{-1} the values of $E_{p,a}$, and $E_{p,c}$ were proportional to the logarithm of the scan rate as indicated by Laviron (Fig. 4b).

The slope of the linear segment is equal to $-2.303\ RT/\alpha_c nF$ for the cathodic and $2.303\ RT/\alpha_a nF$ for the anodic peak. The evaluated values for the coefficients α_c and α_a are 0.57 and 0.41, respectively. Therefore, we consider the average value of 0.58 for α_c (α) and use it in subsequent studies. Sum of transfer coefficient α_c and α_a minimally deviates from its normal value of 1. Similar results have also been reported earlier [11, 31].

A means of $k_s = 3.77 \pm 0.27$ s^{-1} was evaluated from all the extracted experimental data applying Eq. 22 from theoretical paper by Laviron [30]. The value obtained for k_s is lower than those previously reported for electrodes modified by some other compounds with catechol ring [32–35]. This difference originates most probably from the nature of functionalities bound on *o*-hydroquinone ring. However, this value of k_s is comparable or even higher than those reported for some other modified electrodes [35, 36].

The effect of pH on the CMGCE signal was investigated by cyclic voltammetry using a 0.15 M phosphate buffer at various pH values ranging from 2.0 to 12.0. As can bee seen in Fig. 5, the formal potential of the surface redox couple was depends on pH, with a slope of −56.8 mV per pH unit (inset of Fig. 5, curve a) which is very close to the anticipated Nernstian value of −59 mV for two-electron, two-proton process.

The electrochemical behavior of *o*-quinone derivatives has already been discussed theoretically in some details by several authors [37, 38]. It has been shown that the results of theoretical treatments are valid for a surface reaction (bonded species) as well as for a heterogeneous reaction [39]. The validity of the theoretical treatment was also verified experimentally using some adequate systems such as the *p*-benzoquinone–hydroquinone

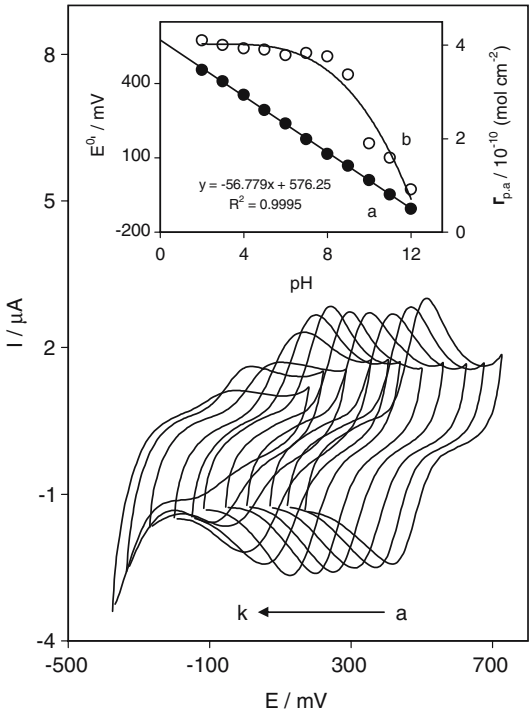

Fig. 5 pH dependence of cyclic voltammetric response of CMGCE at 100 mV s^{-1} in 0.15 M phosphate buffer. The letters *a* to *k* correspond to 2, 3, 4, 5, 6, 7, 8, 9, 10, 11 and 12 pH, respectively. *Inset*: *curve a*, plot of formal potential ($E^{0'}$) versus. pH and *curve b*, variation in surface coverage (Γ) as a function of pH

couple on a platinum electrode [40]. However, the pk_a for catechin was reported ($pk_a = 7.8$) in Salimi et al. [19], so that one would anticipate a change in the slope of $E^{0'}$ versus pH plot around this value. However, such a behavior was not observed in replicate experiments in this work. Since no change in slope was observed, it has to be assumed that no deprotonation of bonded catechin is taking place at this pH. This result is in agreement with those previously reported elsewhere [41].

Another point that should also be mentioned is that the variation in the surface coverage of the modified electrode for pH 2–8 were not dramatic. However, as can be seen in curve b in Fig. 5 inset, for the higher pHs (pH 9–12) a significant decrease in the surface coverage was observed. The loss of coverage could be due to the displacement of surface confined catechin by solvent molecules [42]. The deprotonation of surface-attached materials is also proposed as the origin of coverage decrease by some authors [43]. However, this statement cannot be valid in our case since the surface-bonded catechin remains in its protonated form even at higher pH (see inset in Fig. 5, curve a).

Electrocatalytic activity of the CMGCE toward hydrazine oxidation

The catalytic oxidation of hydrazine by CMGCE was studied by cyclic voltammetry in 0.15 M phosphate buffer, pH = 7.0, in the absence and in the presence of 0.4 mM hydrazine. The electro-oxidation of hydrazine at a bare glassy carbon electrode is shown in Fig. 6d, where cyclic voltammograms was carried out over the potential range −100 mV to 1,000 mV at 20 mV s^{-1}.

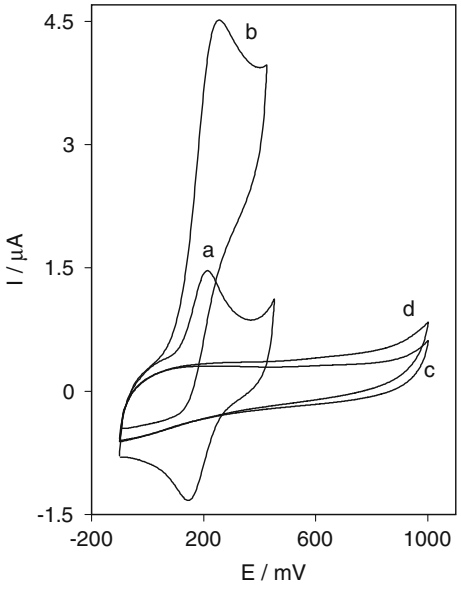

Fig. 6 Current potential curve for **a** CMGCE in 0.15 M phosphate buffer (pH = 7.0) solution and **b** the same electrode in a 0.4 mM hydrazine, pH = 7.0 solution (scan rate: 20 mV s^{-1}). **c** as **a** and **d** as **b** for an unmodified glassy carbon electrode

Direct oxidation of hydrazine shows the representative irreversible wave. The overall oxidation of the hydrazine by the modified electrode is given in Eq. 1.

$$N_2H_4 \rightarrow N_2 + 4H^+ + 4e^- \quad (1)$$

Figure 6a, b shows the representative cyclic voltammograms of a CMGCE in the absence and in the presence of 0.4 mM hydrazine. As expected for an electrocatalytic oxidation there is an increase in the anodic peak current of the $CMGCE_{ox}/CMGCE_{red}$ redox wave (where $CMGCE_{ox}$ is the oxidized form and $CMGCE_{red}$ is the reduced form of the bonded catechin on glassy carbon electrode) in the presence of hydrazine, whereas the reduction peak current has virtually disappeared reflecting the efficiency of the catalytic reaction. The reason is that the hydrazine in the solution diffuse up to the electrode surface and reduces the $CMGCE_{ox}$ to $CMGCE_{red}$. This process increases the anodic peak current, while the cathodic peak current is smaller than in the absence of hydrazine. The overall process according to an EC catalytic mechanism can be expressed as shown in Eqs. 2 and 3.

$$CMGCE_{red} \xrightarrow{k_s} CMGCE_{ox} + 2H^+ + 2e^- \quad (2)$$

$$2CMGCE_{ox} + N_2H_4 \xrightarrow{k'_h} 2CMGCE_{red} + N_2 \quad (3)$$

The rate-determining step is given in Eq. 3 with a rate constant k'_h. Thus, the rate of reaction in Eq. 2 can be considered fast compared to the one in Eq. 3. The catalytic effect can be seen directly when curve a is compared with curve d in Fig. 6. It can be seen that the electrocatalytic-oxidation peak potential (curve b) appear at 225 mV. However, this value is more negative than those previously reported for the other modified electrodes which used in electrocatalytic oxidation of hydrazine [11–18, 44–46] except for only very few other modified electrodes [47]. Thus, a significant decrease in overpotential of hydrazine oxidation at the CMGCE makes it suitable to determine hydrazine by voltammetric detection.

The effect of increasing the hydrazine concentration on the voltammetric response of the CMGCE was also investigated. Figure 7 shows the voltammetric response of the modified electrode on the hydrazine concentration. As can be seen, the plot of the peak current versus hydrazine concentration is constituted of two linear segments with different slopes, corresponding to two different range of substrate concentration. The decrease of sensitivity (slope) in the second linear range (Fig. 7b) is likely to be due to the change in catalytic reaction conditions arising from the formation of nitrogen gas bubbles at the surface of CMGCE as has been reported by others [16]. Indeed, at low hydrazine concentrations, the formed gas, being negligible, has no effect on the diffusion of hydrazine toward the electrode surface (gas evolution unaffected, G.E.U, zone). While, at high concentrations of hydrazine, gas evolution at the electrode surface slackens to some extent the normal

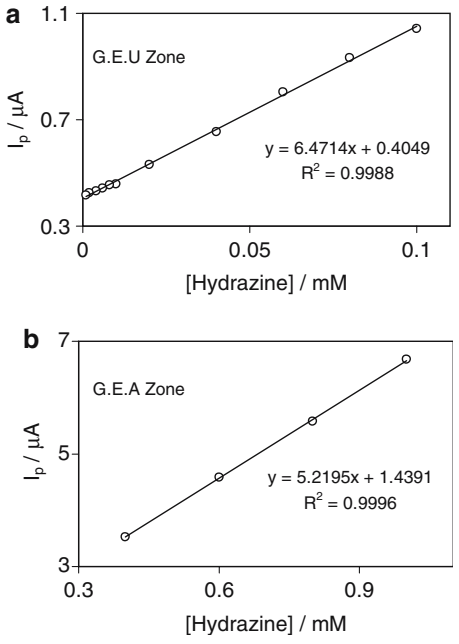

Fig. 7 Variation of catalytic current versus hydrazine concentration in the range of **a** 0.001–0.1 mM and **b** 0.4–1.0 mM, for the CMGCE in 0.15 M phosphate buffer solution. *G.E.U* gas evolution unaffected, *G.E.A* gas evolution affected

diffusion of substrate (gas evolution affected, G.E.A, zone).

Figure 8a shows the cyclic voltammograms of CMGCE at various scan rates obtained in 0.15 M phosphate buffer solution (pH = 7.0) containing 0.11 mM hydrazine. As can be seen, the catalytic oxidation peak potential gradually shifts slightly toward positive potentials with increasing scan rate. However, according to Fig. 8b, curve a, the oxidation peak currents increase linearly with the square root of the scan rate. These results obtained from cyclic voltammetry lead to the conclusion that the overall electrochemical oxidation of hydrazine under these conditions might be under mixed-control from the hydrazine transfer in the solution and the cross-exchange process between hydrazine and redox sites of the catechin film. Moreover, a plot of sweep rate-normalized current ($I_p/v^{1/2}$) versus sweep rate exhibits the characteristic shape typical of a EC catalytic process. For the case of slow sweep rate, v, and large rate constant, k_h', Andrieux and Savent [48] developed a theoretical model for a heterogeneous catalytic reaction:

$$I_{cat} = 0.496nFAC_b(nFDv/RT)^{\frac{1}{2}} \quad (4)$$

where D and C_b are the diffusion coefficient ($cm^2\ s^{-1}$) and the bulk concentration (mol cm^{-3}) of hydrazine, and the other symbols have their usual meanings. Low values of k_h' result in values of the coefficient lower than 0.496 for the constant. Based on extensive computations, a working curve showing the relationship between numerical values of the constant, $I_{cat}(RT)^{1/2}/nFAC_b(nFDv)^{1/2}$, and $\log[k\Gamma(RT)^{1/2}/(nFDv)^{1/2}]$ (Fig. 1b of [48]) is given. The value of k_h' can be calculated from such a working curve. For low scan rates (2–10 mV s^{-1}), we find the value of this constant to be 0.23 for a

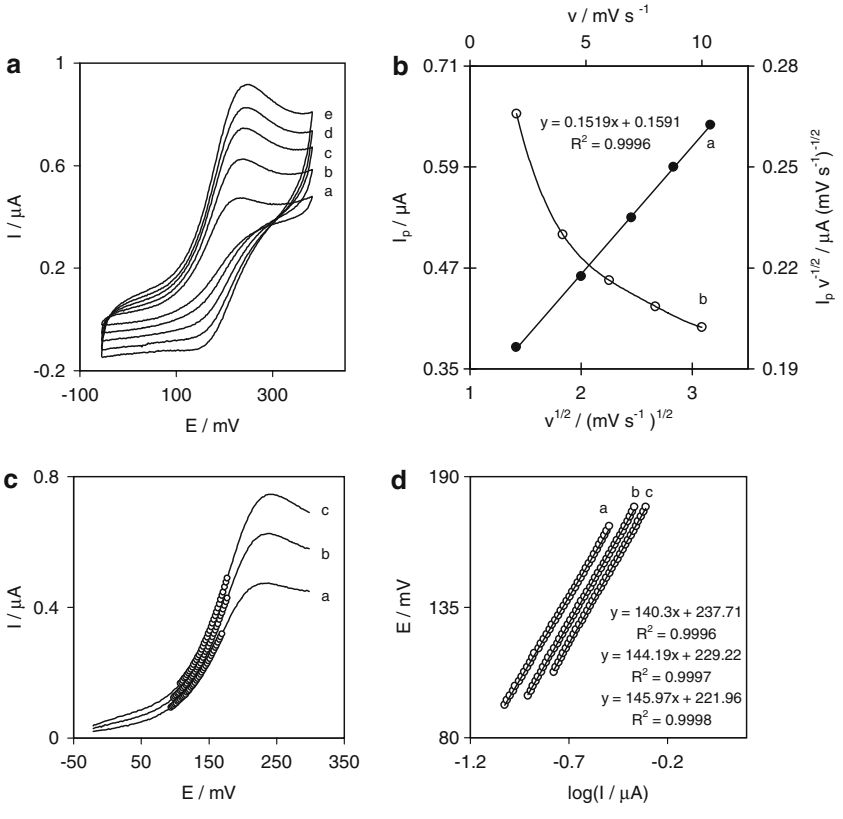

Fig. 8 **a** Cyclic voltammetry of a CMGCE in 0.15 M phosphate buffer solution (pH = 7.0) containing 0.1 mM hydrazine at scan rates: (a) 2, (b) 4, (c) 6, (d) 8 and (e)10 mV s^{-1}. **b** *Curve a*, variation of the electrocatalytic current versus the square root of scan rate and *curve b*, variation of the scan rate normalized current ($I_p/v^{1/2}$) with scan rate. **c** Linear sweep voltammograms derived from the cyclic voltammograms recorded at (a) 2, (b) 4 and (c) 6 mV s^{-1}. The points are the data used in the Tafel plots. **d** Tafel plots derived from linear sweep voltammograms shown in **c**. The equations from top to bottom correspond to curves of a–c, respectively

CMGCE, with coverage of $\Gamma = 5.0\times10^{-10}$ mol cm^{-2}, a geometric area of 0.0314 cm^2 and considering $D = 1.6\times10^{-6}$ cm^2 s^{-1} (this is obtained by chronoamperometry as below), in the presence of 0.11 mM hydrazine. According to the approach of Andrieux and Savent and using Fig. 1b in their theoretical paper [48], we calculated an average value of $k_h' = 9.2\times10^{-4}$ cm s^{-1}. This value is approximately in accordance with that obtained below using chronoamperometry and rotating disk voltammetry. Figure 8c shows the linear sweep voltammograms, which are recorded at different sweep rates. The points show the rising part of voltammograms which is known as Tafel region and is affected by electron transfer kinetics between hydrazine and a CMGCE, assuming the deprotonation of hydrazine as a sufficiently fast step. In the evaluation of kinetic parameters, the Tafel plots were drawn (Fig. 8d), derived from points of the Tafel region of the linear sweep voltammograms in Fig. 8c. The results of polarization studies for electro-oxidation of hydrazine at CMGCE show that for all potential sweep rates, the average Tafel slope is 143.5 mV (Fig. 8d). The value obtained for the average of Tafel slope of the different plots agree well with involvement of one electron transfer in the rate determining step of the electron transfer process, assuming an average charge transfer coefficient of $\alpha = 0.59\pm0.01$ [26]. In addition, the exchange current density, j_0, is obviously readily accessible from intercept of the Tafel plots [26]. The average value obtained for the exchange current density for hydrazine at the CMGCE was found to be 0.80 ± 0.15 μA cm^{-2}.

Rotating disk electrode measurements

In order to elucidate the kinetics of hydrazine oxidation at the CMGCE, rotating disk electrode measurements were also performed with different rotation speed in 0.15 M phosphate buffer (pH = 7.0) containing various concentrations of hydrazine. The results for a 0.05 mM solution of hydrazine at modified electrode surface are shown in Fig. 9a. The Levich plots obtained at 220 mV, for different concentrations of hydrazine, are shown in Fig. 9b. As can be seen, the current increases with increase in rotational speed, but was found to be nonlinear, including kinetic limitation. In addition, and as mentioned earlier, slow electron transfer between the electrodeposited catechin and the electrode can also be discarded as rate-limiting step. Thus, we again conclude that the reaction between hydrazine and the bonded catechin is the sole rate-limiting step [49]. Under these conditions, the catalytic current, I_{cat}, corresponding to the mediated reaction, is a function of the Levich current, I_{Lev}, representing the mass transfer of hydrazine in the solution and the kinetic current, I_k, corresponding to the electron cross-exchange between hydrazine and the catechin redox sites. The value of catalytic reaction rate constant, k_h', between the oxidized form of catechin and hydrazine can be obtained from the Koutecky–Levich plot using the following expressions [26]:

$$\frac{1}{I_{cat}} = \frac{1}{I_{Lev}} + \frac{1}{I_k} \tag{5}$$

which

$$I_{Lev} = 0.62\, nFAv^{-1/6}D^{2/3}\omega^{1/2}C_b \tag{6}$$

$$I_k = nFAk_h'C_b \tag{7}$$

where C_b is the bulk concentration of hydrazine in solution (mol cm^{-3}), ω is the angular frequency of rotation (rad s^{-1}), ν is the kinematic viscosity (cm^2 s^{-1}) and all other symbols having their conventional meanings. From the above equation, it is apparent that the value of k_h' can be determined from the intercept of the plot of I_{cat}^{-1} versus $\omega^{-1/2}$ (Fig. 9c). It was found that k_h'

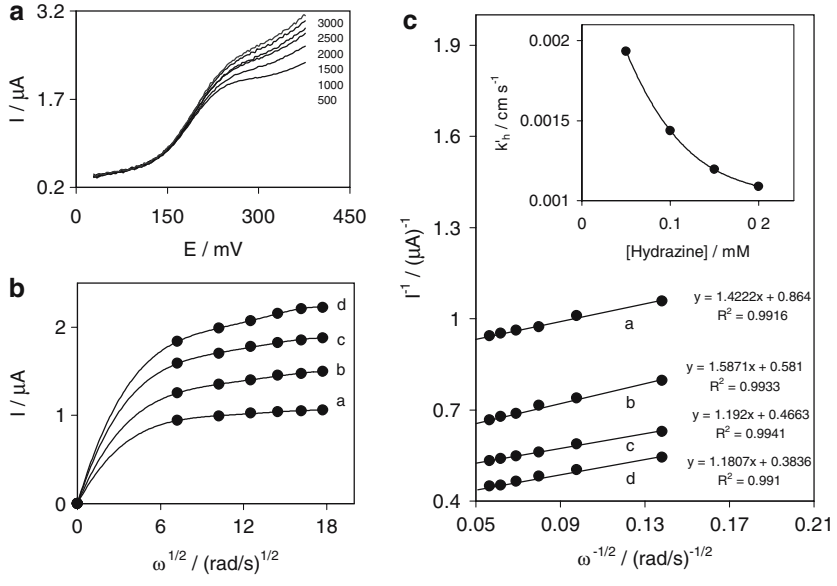

Fig. 9 **a** Voltammograms of a catechin modified glassy carbon rotating disk electrode in 0.15 M phosphate buffer (pH = 7.0) containing 0.05 mM hydrazine at various rotation rates indicated for each voltammograms. **b** Levich plots constructed from the modified RDE voltammograms of solutions with (a) 0.05, (b) 0.10, (c) 0.15, (d) 0.20 mM hydrazine and using currents for E_{disc} = 220 mV. **c** Koutecky–Levich plots obtained from Levich plots shown in **b**. *Inset* shows the plot of catalytic rate constant versus concentration of hydrazine

decreases significantly with increase in the bulk concentration of hydrazine (Fig. 9c, inset). A similar observation has been reported previously for the electrocatalytic–oxidation of hydrazine at electrodes modified with different mediators [16, 18]. We believe, as mentioned earlier, that this is due to an increase in the production of nitrogen on the bounded catechin, with the increase in the hydrazine concentration in solution. The nitrogen molecules may adsorb on the catechin film and thus apparently diminish the number of catalytically active sites. This leads to a decrease of the rate constant observed. This observation also provides additional evidence against the restricted access of the hydrazine, as the rate-limiting step. From the values of the intercept, an average value of k_h' was found to be 1.4×10^{-3} cm s^{-1}, which is approximately similar to that determined from the cyclic voltammetric measurements.

Chronoamperometric and amperometric studies

The catalytic oxidation of hydrazine by a CMGCE was also studied by chronoamperometry. Chronoamperograms obtained at different concentration of hydrazine at a potential step of 300 mV are depicted in Fig. 10a. With the addition of hydrazine, there was an increase in the anodic current. Figure 10b shows, similarly to the case of cyclic voltammetry, the plot of the fixed time current, the current measured after 45 s, versus hydrazine concentration constituted from two linearly segments with different slopes, corresponding to two different ranges of 5–60 and 60–300 μM hydrazine. As mentioned above, we defined these by G.E.U and G.E.A zones for low and high concentrations of hydrazine, respectively. For hydrazine concentrations above 0.30 mM, the measured current is also linearly proportional to the concentration, but with a decreased sensitivity (slope). It seems that at higher hydrazine concentration, the catalytic oxidation of substrate occurs with some limitation with constant effect. Such a behavior, as mentioned before, may be due to the effect of the nitrogen gas bubbles formation at the modified electrode surface. Indeed, the change in the slopes of the calibration plots arise from the change of the apparent diffusion coefficient of hydrazine, which is smaller when the electrode surface is almost covered by nitrogen bubbles.

Chronoamperometry was also used for the measurement of the catalytic rate constant, k_h', of the chemical reaction between hydrazine and the surface bounded catechin. Using chronoamperometry method, k_h' can be evaluated according to the method of Galus [50]:

$$I_{cat}/I_l = \gamma^{1/2}[\pi^{1/2}\mathrm{erf}(\gamma^{1/2}) + \exp(-\gamma)/\gamma^{1/2}] \quad (8)$$

where $\gamma = k_h' C_b t$ (C_b is the bulk concentration of hydrazine, t is the time elapsed, s) is the argument of the error function, I_{cat} is the catalytic current of CMGCE in the presence of hydrazine and I_l is the limited current in the absence of hydrazine. When $\gamma > 1.5$, the reaction zone is in the pure kinetic region and Eq. 8 can be reduced to:

$$I_{cat}/I_l = \pi^{1/2}\gamma^{1/2} = \pi^{1/2}(k_h' C_b t)^{1/2} \quad (9)$$

On the slope of the I_{cat}/I_l versus $t^{1/2}$ plot, k_h' can be obtained for a given hydrazine concentration. The advantage of this method is that is unnecessary to know the diffusion coefficient of substrate or the electrode area. Such a plot was constructed from the chronoamperograms of CMGCE in the absence and presence of 0.005 mM hydrazine (inset in Fig. 10a), from whose we calculated a catalytic rate constant of 1.2×10^{-3} cm s^{-1} for hydrazine. This value is approximately similar to those determined from cyclic voltammetric and rotating disc voltammetric measurements. Also this value is comparable with those previously reported for the electrocatalytic oxidation of hydrazine at electrode modified with other mediators [18].

Chronoamperometry was used for measurement of the diffusion coefficient of hydrazine. For an electroac-

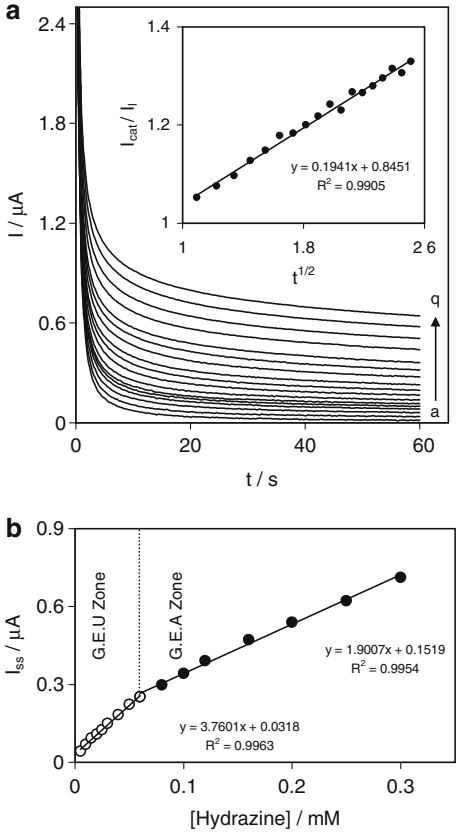

Fig. 10 **a** Chronoamperometric response of a CMGCE in 0.15 M phosphate buffer solution (pH = 7.0) containing different concentrations of hydrazine for a potential step of 300 mV. The letter (a) to (q) correspond to 0, 0.005, 0.01, 0.015, 0.02, 0.025, 0.03, 0.04, 0.05, 0.06, 0.08, 0.10, 0.12, 0.16, 0.20, 0.25 and 0.30 mM hydrazine, respectively. *Inset* shows the variation of I_{cat}/I_l vs. $t^{1/2}$ which I_l and I_{cat} derived from the data of chronoamperograms (a) and (b) respectively. **b** Variation of chronoamperometric current at t = 45 s versus hydrazine concentration. *G.E.U* gas evolution unaffected, *G.E.A* gas evolution affected

tive material (hydrazine in this case) with a diffusion coefficient, D, the current for the electrochemical reaction (at a mass transport limited rate) is described by Cottrell equation [26]:

$$I = nFAD^{1/2}C_b/\pi^{1/2}t^{1/2} \quad (10)$$

The plot of I versus $t^{-1/2}$ will be linear, and from the slope, the value of diffusion coefficient can be obtained. We have carried out such studies at various hydrazine concentrations, for a CMGCE. Figure 11 shows the experimental plots with the best fits for different concentration of hydrazine employed. The slopes of the resulting straight lines were then plotted versus the hydrazine concentration (inset in Fig. 11), from whose slope we calculate a diffusion coefficient of 1.6×10^{-6} cm^2 s^{-1} for hydrazine. However, the calculated value of the diffusion coefficient is close to the value reported elsewhere [18] but it is lower than that reported by others [51].

On the basis of voltammetric results described in previous section, the CMGCE has excellent and strong electrocatalytic properties and facilities at low potential amperometric measurements of hydrazine. Also, amperometry under stirred conditions has a much higher current sensitivity than cyclic voltammetry and it can be used to estimate the lower limit of detection of hydrazine at CMGCE. Figure 12a shows amperograms which were recorded for a rotating CMGCE (rotation speed 2,500 rpm), under conditions where the potential was kept at 300 mV in 0.15 M phosphate buffer solution (pH = 7.0). As can be seen, during successive addition 10.0 and 20.0 μM of hydrazine (Fig. 12a, curve b) even 2.0 μM (Fig. 12a, curve a) a well defined response was observed. For each addition of hydrazine within a response time less than 1 s, a sharp rise in the current was observed.

The dependence of the current on the hydrazine concentration, in the range of 2.0–58.4 μM and 58.4–237.2 μM, is shown in Fig. 12b. The curves of a and b of this figure clearly shows that plot of current versus hydrazine concentration is constituted from two linear segments with different slopes, corresponding to two different ranges of substrate concentration. The decrease of sensitivity (slope) in the second linear range (Fig. 12b, curve b) can also be considered as a result of gas evolution effect on the diffusion of hydrazine toward the electrode surface.

A calibration plot of average amperometric current of three replicate measurements versus hydrazine concentration, in the range of 2.0–10.0 μM (not shown), was used to estimate the lower limit of detection of hydrazine at a CMGCE. The linear least square calibration curve over the above range had slope of 0.0085 μA μM^{-1} (sensitivity) and correlation of 0.9997. According to the method mentioned in the ref. [52], the lower detection limit, C_m, was obtained using of the equation of $C_m = 3s_{bl}/m$, where s_{bl} is the standard deviation of the blank response (μA) and m is the slope of the calibration plot (μA μM^{-1}). In this experiment, 18 replicate measurements was performed on the blank solution and the resulting data are then treated statistically to obtain $s_b = 4.68\times10^{-4}$ μA. From the analysis of these data, we estimate that the limit of detection of hydrazine is of the order of 0.165 μM. Also, the average

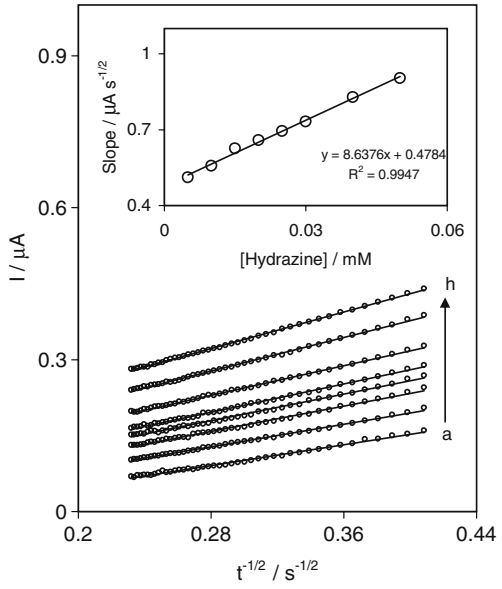

Fig. 11 Plots of I versus $t^{-1/2}$ obtained from chronoamperometric experiments for a CMGCE in 0.15 M phosphate buffer solution (pH = 7.0) containing different concentration of hydrazine. The letters a to h correspond to 0.005, 0.01, 0.015, 0.02, 0.025, 0.03, 0.04, 0.05 mM hydrazine, respectively. *Inset* shows the slope of linear segments against the hydrazine concentration

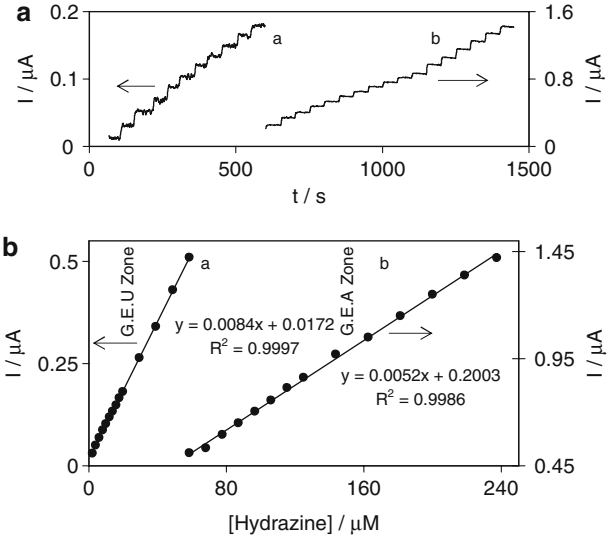

Fig. 12 **a** Amperometric response at rotating CMGCE (rotation speed 2,500 rpm) held at 300 mV in 10 mL, 0.15 M phosphate buffer (pH = 7.0) for (a) successive 10 addition of 20 μL hydrazine 1.0 mM and (b) successive 11 addition of 20 μL hydrazine 5.0 mM and successive 6 addition of 20 μL hydrazine 10.0 mM to (a). **b** Variation of amperometric current versus hydrazine concentration in the range of (a) 2.0–58.4 μM and (b) 58.4–237.2 μM. *G.E.U* gas evolution unaffected, *G.E.A* gas evolution affected

amperometric current (μA) and the precision estimated in terms of relative standard deviation (%RSD) for 25 repeated measurements ($n = 25$) of 40.0 μM hydrazine at an applied potential of 300 mV, on a CMGCE were 0.341 ± 0.016 μA and 4.7%, respectively.

Square-wave voltammetry measurements

The effect of increasing concentration of hydrazine on the voltammetric response of the CMGCE was also investigated by square-wave voltammetry. Inset in Fig. 13 shows the square-wave voltammograms, SWV, for different concentration of hydrazine. Upon the addition of hydrazine, there was an enhancement in the anodic peak current. The dependence of the peak current on the hydrazine concentration is shown in Fig. 13. It clearly shows that the SWV current response is linearly dependent on the concentration of hydrazine between 0.5–60.0 μM and 60.0–1000.0 μM with slope of 0.03984 and 0.0078 μA μM^{-1}, respectively. Similarly to the previous cases, this plot exhibit obviously two separate linear correlations, each corresponding to a given concentration range. As mentioned above, we defined these by G.E.U and G.E.A zones for low and high concentrations of hydrazine respectively.

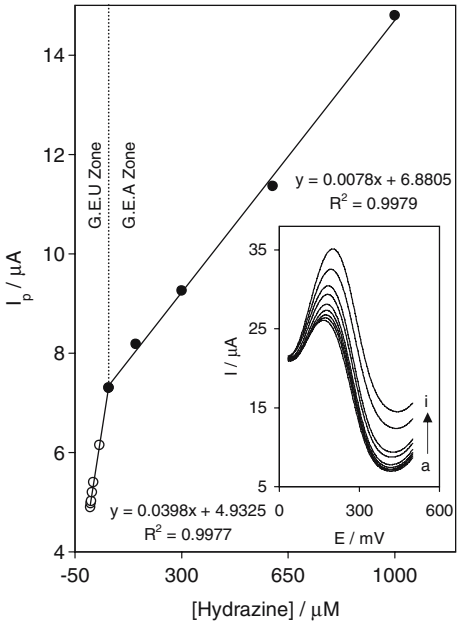

Fig. 13 Plot of peak current of the square wave voltammograms versus hydrazine concentration at the CMGCE. *Inset* shows the square wave voltammograms at a CMGCE in 0.15 M phosphate buffer solution (pH = 7.0) containing different concentration of hydrazine. The letters of a to i correspond to 0.5, 6.0, 10.0, 30.0, 60.0, 100.0, 300.0, 600.0 and 1000.0 μM hydrazine. Square wave amplitude: 100 mV; Square wave frequency: 10 Hz; step potential: 2.55 mV. *G.E.U* gas evolution unaffected, *G.E.A* gas evolution affected

Conclusions

The results obtained here show that the activated glassy carbon electrode can be modified easily by catechin during potential recycling. The optimum conditions for the electrode surface modification are also precise and the stability of such an electrode, as well as its surface coverage has been determined. Cyclic voltammetry was used to investigate the redox properties of this modified electrode at various solution pH values and at various scan rates. The pH dependence of the modified electrode was found to be −56.8 mV/pH, in the pH range 2.0–12.0, which is close to the anticipated Nernstian dependence of −59 mV/pH.

The modified electrode exhibits potent and persistent electrocatalysis for hydrazine oxidation and it offers a marked decrease in the overvoltage for hydrazine oxidation. The currents obtained in cyclic voltammetry, chronoamperometry, amperometry, and square-wave voltammetry are diffusion controlled for low concentrations of hydrazine, while at high substrate concentrations the currents are significantly decreased most probably because of nitrogen gas evolution. The diffusion coefficient of hydrazine was calculated as 1.6×10^{-6} cm^2 s^{-1} for the experimental conditions, using chronoamperometric results. Finally, the kinetic parameters such as electron transfer coefficient, α, and catalytic reaction rate constant, k_h', were also determined using various electrochemical approaches.

References

1. Schessl HW (1995) In: Othmer K (ed) Encyclopedia of chemical technology, 4th edn, vol 13. Wiley, New York, pp 560
2. Choudhary G, Hansen H (1998) Chemosphere 37:801
3. Amlathe S, Gupta VK (1988) Analyst 113:1481
4. Zhi Z, Ren J, Qing Z (1992) Gaoden Xuexiao Huaxue Xuebao 14:1710
5. Ensafi AA, Naderi B (1997) Microchem J 56:269
6. Wang Y (1992) Shanghai Huanjing Kexue 11:28
7. Preece NE, Forrow S, Ghatineh S, Langley GJ, Timbrell JA (1992) J Chromatogr 573:227
8. Poster TJ, Vajgand VJ, Antonijeic NV (1983) Mikrochim Acta 3:203
9. Mo JW, Ogorevc B, Zhang XJ, Pihlar B (2000) Electroanalysis 12:48
10. Fiala ES, Kulakis CJ (1981) J Chromatogr 214:229
11. Li X, Zhang S, Sun C (2003) J Electroanal Chem 553:139
12. Pingarrón JM, Ortiz Hernández I, González-Cortés A, Yáñez-Sedeño P (2001) Anal Chim Acta 439:281
13. Yang M, Li HL (2001) Talanta 55:479
14. Casella IG, Guascito MR, Salvi AM, Desimoni E (1997) Anal Chim Acta 354:333
15. Golabi SM, Noor-Mohammadi F (1998) J Solid State Electrochem 354:333
16. Scharf U, Grabner EW (1996) Electrochimica Acta 41:233
17. Wang W, Chen Q, Cepria G (1996) Talanta 43:1387
18. Golabi SM, Zare HR (1999) J Electroanal Chem 465:168
19. Salimi A, Abdi K, Khayatian G (2004) Microchim Acta 144:161
20. Middleton E Jr, Kandaswami C, Harborne JB (1986) In the flavonoids, chap 15. Chapman and Hall, London

21. Thompson RS, Jacques D, Haslam E, Tanner RJN (1972) J Chem Soc Perkin Trans 1:1387
22. Miller JN, Miller JC (2000) Statistics and chemometrics for analytical chemistry, 4th edn. Pearson Education Ltd, Harlow
23. Nematollahi D, Golabi SM (1996) J Electroanal Chem 405:133
24. Golabi SM, Nematollahi D (1997) J Electroanal Chem 420:127
25. Schreurs J, Van der Berg J, Wonders A, Barendrecht E (1984) Rec Trav Chim Pays-Bas 103:251
26. Bard AJ, Faulkner LR (2001) Electrochemical methods, fundamentals and applications. Wiley, New York
27. Garton L, Torstensson A, Jaegfeldt H, Johansson G (1984) J Electroanal Chem 161:103
28. Florou AB, Prodromidis MI, Tzouwara-Karayanni SM (1998) Electroanalysis 10:1261
29. Ju H, Shen C (2001) Electroanalysis 13:789
30. Laviron E (1979) J Electroanal Chem 101:19
31. Sharp M, Petersson M, Edström K (1979) J Electroanal Chem 95:123
32. Zare HR, Golabi SM (1999) J Electroanal Chem 464:14
33. Golabi SM, Zare HR (2000) J Solid State Electrochem 4:87
34. Golabi SM, Zare HR, Hamzehloo M (2002) Electroanalysis 14:611
35. Jaegfeldt H, Kuwana T, Johansson G (1983) J Am Chem Soc 105:1805
36. Jaegfeldt H, Torstensson ABC, Gorton LGO, Johansson G (1981) Anal Chem 53:1979
37. Laviron E (1983) J Electroanal Chem 146:15
38. Kojima H, Bard AJ (1975) J Am Chem Soc 97:6317
39. Laviron E (1983) J Electroanal Chem 146:1
40. Laviron E (1984) J Electroanal Chem 164:213
41. Janeiro P, Brett AMO (2004) Anal Chim Acta 518:109
42. Horspool WM, Smith PI, Tedder JM (1972) J Chem Soc Perkin Trans 1024
43. Lorenzo E, Sanchez L, Pariente F, Tirado J, Abruna HD (1995) Anal Chim Acta 309:79
44. Narayanan SS, Scholz F (1999) Electroanalysis 11:465
45. Li T, Wang E (1997) Electroanalysis 9:1205
46. Gong X, Zhou YK, Li HL (2001) Talanta 55:1103
47. Niu L, You T, Gui JY, Wang E, Dong S (1998) J Electroanal Chem 448:79
48. Andrieux CP, Saveant JM (1978) J Electroanal Chem 93:163
49. Rocklin RD, Murray RW (1981) J Phys Chem 85:2104
50. Galus Z (1994) Fundamentals of Electrochemical Analysis. Ellis Horwood, New York
51. Wang BC, Cao XQ (1991) J Electroanal Chem 309:147
52. Skoog DA, Holler FJ, Nieman TA (2001) Principles of instrumental analysis, 5th edn. Harcourt Brace, Philadelphia